Sinter-Hardening Response of a Lean Sinter-Hardening Alloy

Suresh Shah, Gilbert Schluterman, Jr., PMT, and Gregory Falleur, PMTII
AAM Powertrain
Subiaco, AR 72865

Kylan McQuaig, Katie Jo Sunday, and Sunil Patel
Hoeganaes Corporation
Cinnaminson, NJ 08077

Abstract

Sinter hardening alloys are widely known as an alternative to eliminate the requirement for a separate heat treat operation. In addition to the improved economics inherent with less processing in some applications, the process results in reduced dimension variation as compared to batch heat and quench processes.

This paper compares physical properties of the robust sinter hardening alloy FLC2-4808 to a leaner alloy. In addition to data from standard test bars, properties from processing medium-sized sprockets under production conditions were evaluated.

Introduction

Over the years, there have been constant advancements in the powder metallurgy (PM) industry aimed at reducing costs and processing steps while simultaneously increasing the achievable properties of PM materials. Two of the most substantial improvements that can be made to the mechanical properties of a PM part are compacting to higher density and using enhanced sintering and heat treating techniques to achieve a hardened microstructure.

Through the development of advanced furnace technology, increasing the cooling rate of a standard sintering furnace now makes it possible to "harden" PM parts by forming a martensitic microstructure without the need for additional heat treatment processing. Due to its cost advantages, reduced processing steps, and lower dimensional distortion, sinter-hardening technology has been pursued and perfected over the past few decades [1-10].

While it has been shown that sinter-hardening is beneficial from a processing perspective, appropriate materials are necessary in order to properly utilize this technology. Material "hardenability" is a term used to quantify a given material's ability to transform to martensite upon cooling from its austenitization temperature. Common alloying elements in steel such as manganese, chromium, molybdenum, copper, and nickel can provide substantial increases to material hardenability, but with potentially negative effects in terms of material cost, compressibility, and sinter-ability. In order to fulfill the needs of the industry, Hoeganaes Corporation developed a robust sinter-hardening material, Ancorsteel 737 SH, corresponding to MPIF standard FL-4800 type materials. During this development work, Baran et al. discussed the benefits and potential drawbacks of these various alloying elements at length as shown in Figure 1 below [1].

	Hardenability Factor	Effect on Compressibility	Affinity for Oxygen
Higher ↓ Lower	Manganese	Copper	Manganese
	Chromium	Nickel	Chromium
	Molybdenum	Chromium	Nickel
	Copper	Manganese	Molybdenum
	Nickel	Molybdenum	Copper

Figure 1: Ranking of alloying elements in prealloyed PM materials [1].

Since 2000, several other grades of material have been developed and their degrees of hardenability have been characterized using various methods including jominy bars, CCT curves, metallographic analysis, and apparent hardness measurement on sintered slugs [2-7]. In 2010, Sokolowski and Lindsley evaluated many of the standard sinter-hardening grades via jominy testing, including Ancorsteel 737 SH and a newly developed leaner grade, Ancorsteel 721 SH [2]. The jominy hardenability curves for both of the materials compared to other common PM sinter-hardening grades are shown in Figure 2. As seen in the figure, Ancorsteel 737 SH and 721 SH are two of the most hardenable materials commercially available at this time.

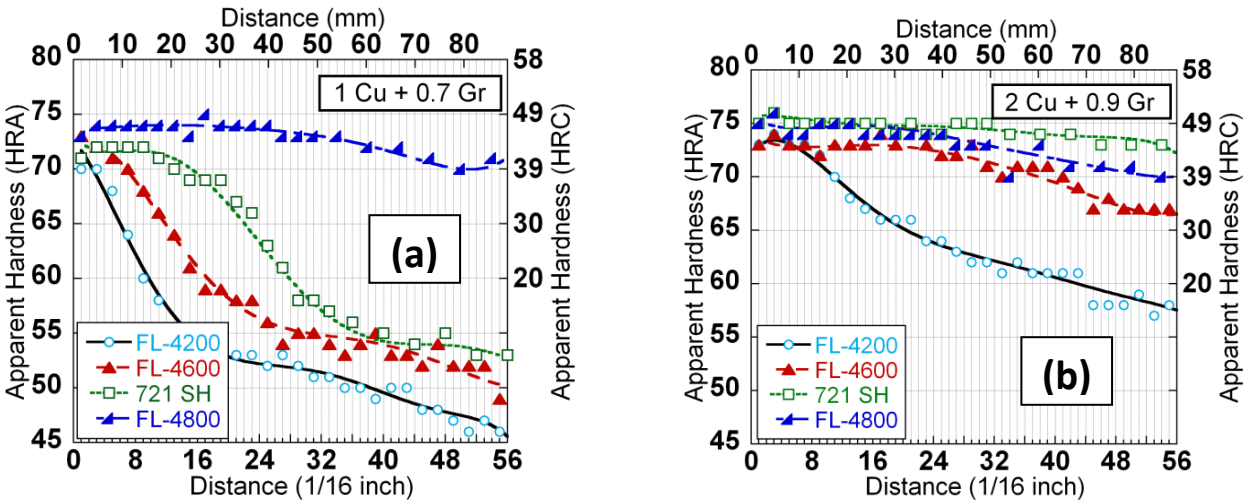

Figure 2: Jominy hardenability curves for common sinter-hardening PM alloys with (a) 1% Cu-0.7% graphite addition and (b) 2% Cu-0.9% graphite addition [2].

While the benefits of sinter-hardening are apparent, increasing the prealloyed content of the material also leads to a decrease in material compressibility, as a general trend. Because of the important link between density and mechanical properties of sintered PM steels, there is a strong motivation to achieve density levels as high as possible. While forging and double-press/double-sinter (DPDS) processing routes are viable options, they also increase the number of processing steps and can lead to higher production costs.

Warm compaction and warm die compaction lubricant systems allow for compaction of high density parts without any additional processing steps. The benefits of these lubricant systems are well documented, resulting in a substantial increase in achievable mechanical properties compared to lower density alternatives. Material strength and apparent hardness have been shown to increase in a linear manner with density in PM materials, while the increase in ductility and impact toughness is even more substantial [10-12].

The following study utilizes the benefits of both sinter-hardening and high density processing. The use of these key technologies allows for the production of a high density, fully martentisic PM part without any secondary processing steps. Through laboratory testing and production trials, the effects of density, material type, and final part size are evaluated in regards to hardenability and sintered mechanical properties.

Experimental Procedure

Material Preparation – Hoeganaes Corporation (Milton, PA)

Commercially available powders from Hoeganaes Corporation, Ancorsteel 737 SH and Ancorsteel 721 SH were used as the base alloys in this study. Ancorsteel 737 SH was used as the base material for the MPIF standard FLC2-4808 material and Ancorsteel 721 SH was used as the base material for a comparable lower alloy composition, which has no current MPIF designation. The nominal compositions of the mixes are shown in Table 1 in mass %. All mixes were made with 0.80 mass % Asbury type 3203H graphite, 2.0 mass % American Chemet 1700H fine copper, and 0.40 mass % AncorMax 225 proprietary high density lubricant from Hoeganaes Corporation.

Table 1: Nominal compositions of alloys (prealloyed unless otherwise noted)

Mix Designation	Manganese (wt%)	Nickel (wt%)	Molybdenum (wt%)	Copper* (wt%)	Carbon* (wt%)
FLC2-4808	0.40	1.40	1.25	2.10	0.80
Ancorsteel 721 SH	0.40	0.50	0.90	2.50	0.80

*Both mixes contain 2.0 mass % admixed copper and 0.80 mass % admixed graphite

Laboratory Testing – Hoeganaes Corporation, Research & Development (Cinnaminson, NJ)

Transverse rupture (TR) strength bars were compacted to green densities of 7.0 and 7.2 g/cm^3 at a die temperature of ~110 °C (225 °F) in order to determine the static mechanical properties of each mix. All test bars were sintered in an Abbott continuous-belt furnace at 1120 °C (2050 °F) for 20 minutes at temperature in a mixed atmosphere of 90 volume % nitrogen and 10 volume % hydrogen. Standard furnace cooling and accelerated cooling were used with approximate cooling rates of 0.7 °C/s and 1.6 °C/s, respectively, from austenitization temperature. All samples were then tempered at 205 °C (400 °F) for one hour in air prior to mechanical testing. The sintered density, dimensional change, and apparent hardness were determined on TR bars following MPIF Standards 42, 43, and 44. TR strength testing adhered to MPIF Standard 41 [13]. Sintered carbon values were measured using a Leco 200 carbon-sulfur combustion gas analyzer with reference standards run before and after test samples.

The effect of sample size on final martensite content was studied for each material on cylindrical slugs pressed to a density of 7.0 g/cm^3, a height of approximately 2.5 cm (1 inch), and increasing diameters of 2.5 and 3.8 cm (1.0 and 1.5 inches). The relative sizes of the cylindrical slugs are shown in Figure 3. The samples were then sinter-hardened and tempered using the methods described previously. These samples were then ground and polished using standard metallographic preparation, and the microstructures were observed at the center of each specimen.

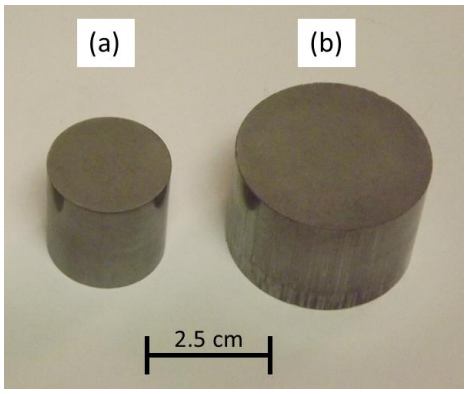

Figure 3: Relative sizes of the final sintered slugs with diameters of 2.5 cm (a) and 3.8 cm (b).

Production Capability – AAM Powertrain (Subiaco, AR)

In addition to laboratory testing, short production trials were performed using sprockets in order to understand the effect of part size on material hardenability and properties under standard production conditions. The sprocket geometry used for the production portion of this study is shown in Figure 4, with a maximum outer diameter (from tooth tip-to-tooth tip) of approximately 7.5 cm. Sprockets were pressed at various heights in order to change individual part weight and overall furnace loading. Sprockets were compacted with masses of 250, 500, 750 grams and to green density levels of 7.0 and 7.2 g/cm^3 using a die temperature of ~100 °C (210 °F). From each combination of density, mass, material type, and sintering conditions, a minimum of 20 parts were compacted. The sprockets were then sintered at AAM Powertrain in a standard production furnace at 1120 °C, with an atmosphere of 95 volume % nitrogen and 5 volume % hydrogen, and at two different cooling rates. The cooling rates were measured using a furnace profile and calculated as shown in Figure 5 through the vital temperature range of 315-650 °C. For each combination of material and density, a standard furnace cooling rate of approximately 0.4 °C/s was used as well as an accelerated cooling rate of 1.2 °C/s. Tempering was performed on all samples at 175 °C (350 °F) for 1.5 hours in air using a batch process. These sprockets were used to evaluate apparent hardness and core microstructures. Microstructural analysis was performed at Hoeganaes Corporation.

Figure 4: Sprocket geometry used for production portion of the study, showing parts (left to right) pressed with mass of 250, 500, and 750 grams.

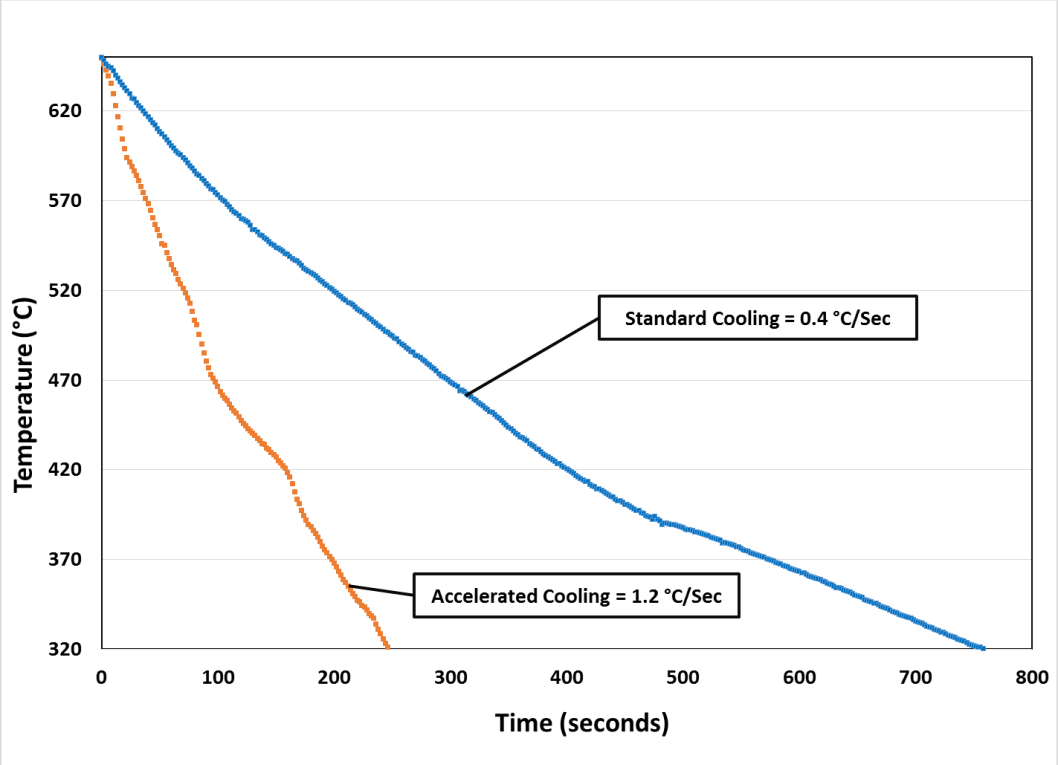

Figure 5: Measured temperature vs. time for calculating both cooling rates during production study.

Results

Laboratory Testing Results

Prior to any compaction of sample bars, both materials were first tested for basic powder properties including apparent density and hall flow, as shown in Table 2. As expected of binder-treated material, both powder samples were found to have a relatively high apparent density of approximately 3.20 g/cm^3 and low Hall flow values of 24 s/50g. Both powder samples were observed to have similar fill and flow characteristics.

Table 2: Powder properties of both materials

Mix Designation	Apparent Density (g/cm^3)	Hall Flow (s/50g)
FLC2-4808	3.22	24
Ancorsteel 721 SH	3.20	24

Mechanical properties were then tested in a laboratory setting to compare the behavior of each alloy at multiple densities on a small scale. The sintered properties of each alloy are shown in Table 3 at 7.0 and 7.2 g/cm^3 nominal green density levels. The bars were sintered with a standard furnace cooling rate of ~0.7 °C/s and tempered for one hour. As expected, the more highly alloyed FLC2-4808 showed an increase in mechanical properties compared to the Ancorsteel 721 SH material. For both materials, there was an increase in apparent hardness and approximately 15% higher strength when density was elevated from 7.0 to 7.2 g/cm^3. The benefits of high density are quite apparent in these results, allowing a leaner sinter-hardening material at the same cooling rate to achieve equal strength simply through an increase in compaction tonnage. The etched microstructures of these TR strength bars, seen in Figure 6, correlate well with these results. At a standard furnace cooling rate, the highly alloyed FLC2-4808 material shows a microstructure that is almost completely transformed to martensite. Meanwhile, the leaner alloy still displays a high percentage of bainite. It is the increased percentage of tempered martensite that results in the higher strength and hardness in the FLC2-4808 material.

Table 3: TRS properties of both materials

Mix Designation	Green Density (g/cm^3)	Dimensional Change (%)	TRS (MPa)	Apparent Hardness (HRC)
FLC2-4808	7.0	0.35	1,627	37
	7.2	0.43	1,882	40
Ancorsteel 721 SH	7.0	0.38	1,427	26
	7.2	0.43	1,655	30

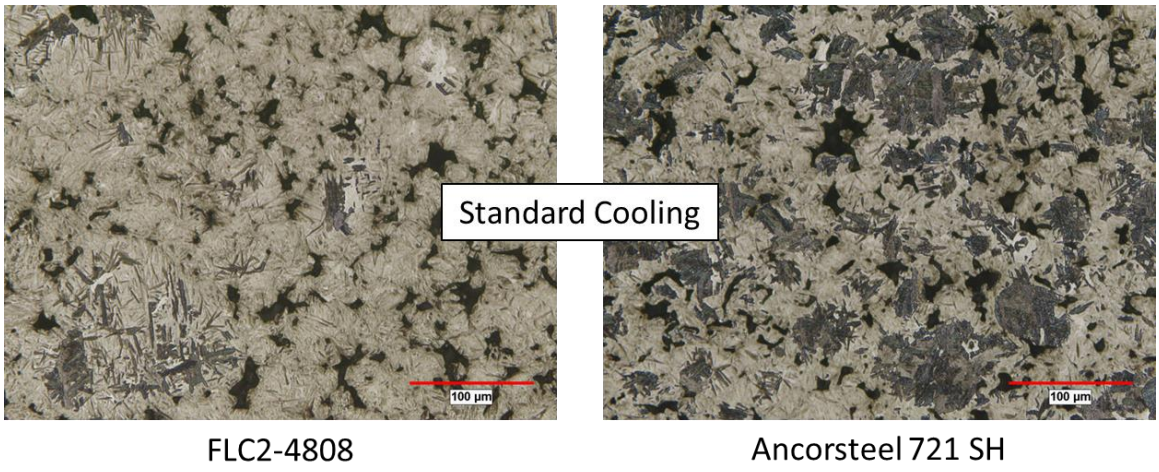

Figure 6: Etched microstructures of TR strength samples at a standard furnace cooling rate.

In order to evaluate the hardenability of each material and help demonstrate the role of sample size, these two alloys were also compacted into cylindrical slugs approximately 3.8 cm in diameter and 2.5 cm in height. They were sintered in the same manner as the above sample bars and sectioned to determine the amount of martensite formation in the core of each slug. As shown in Figure 7, the FLC2-4808 again showed a higher amount of martensite compared to the leaner material, which had an even higher percentage of bainite than was evident in the smaller TRS bars. It is clear that the larger slug size resulted in a slower cooling rate at the core of both alloys, leading to a reduction in martensite content in both materials. This, in turn, leads to lower apparent hardness and strength values.

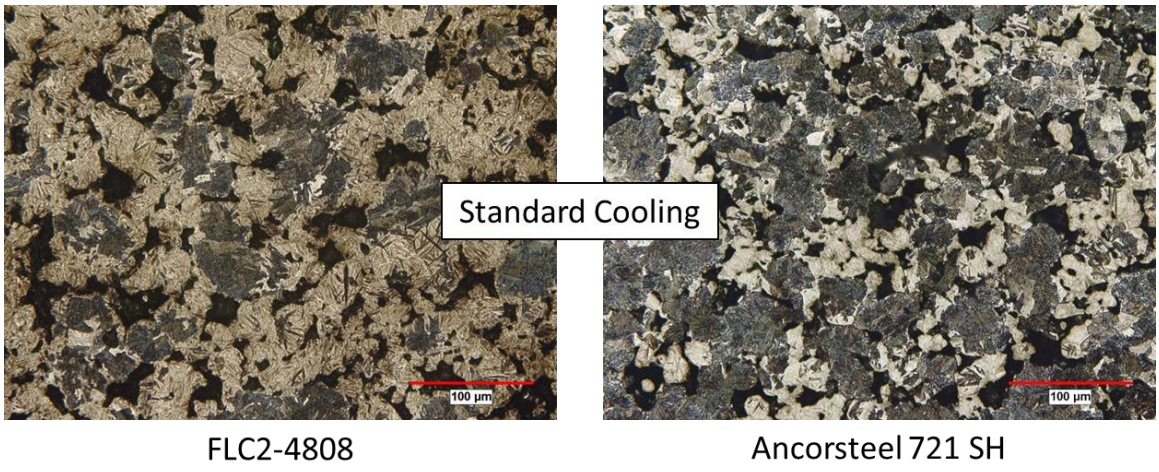

Figure 7: Etched microstructures of 3.8 cm diameter slugs at a standard furnace cooling rate.

Production Results

To fully understand the response of each material under production conditions, trials were performed at AAM Powertrain on medium-sized sprockets, as shown previously in Figure 4. While all other compaction conditions and part density were held constant, the fill was increased to create three distinct parts heights, corresponding to final sprocket weights of approximately 250, 500, and 750 grams. Despite an identical overall sprocket profile and part dimensions, increasing the sprocket height and weight leads to a lower cooling rate under the same sintering conditions. While the direct distance for heat removal remains unchanged in each individual part, the increase in weight and overall furnace loading makes heat removal far more difficult for a given batch of parts.

This is evident when comparing the apparent results from both materials at all three sprocket heights, shown in Table 4. Each material was compacted into sprockets at two green density levels, three sprocket weights, and was sintered using two different cooling rates. There are several trends that become immediately evident. As expected, increasing alloy content and/or green density leads to an increase in apparent hardness under any sintering conditions. Increasing the cooling rate in the furnace from approximately 0.4 to 1.2 °C/s also led to higher apparent hardness values in each condition, but this increase was far more dramatic for the lower alloyed Ancorsteel 721 SH material. While the FLC2-4808 appears far superior under a standard cooling rate due to the inherent hardenability of the alloy, there is little difference in sprocket apparent hardness between these two alloys when an accelerated furnace cooling rate is used.

Table 4: Apparent hardness results from sprockets made of each material at various green density, weight, and cooling rate combinations

Mix Designation	Green Density (g/cm^3)	Part Weight (g)	Std. Cooling Apparent Hardness (HRC)	Acc. Cooling Apparent Hardness (HRC)
FLC2-4808	7.0	250	32	37
		500	24	38
		750	23	37
	7.2	250	37	42
		500	28	41
		750	28	43
Ancorsteel 721 SH	7.0	250	15	37
		500	10	35
		750	9	32
	7.2	250	20	41
		500	16	41
		750	16	39

These trends are shown graphically in Figures 8 and 9, which display apparent hardness vs. sprocket weight for each material and cooling rate combination. As shown in each figure, FLC2-4808 has a significantly higher apparent hardness under standard furnace cooling conditions. An increased cooling rate made this difference negligible at both sprocket densities. This was especially true at the smallest sprocket size. The 250 g sprockets with the highest cooling rate had nearly identical apparent hardness regardless of alloy type. While the difference between alloys became more apparent with increasing sprocket height and weight, it was still minor when compared to the standard cooling conditions.

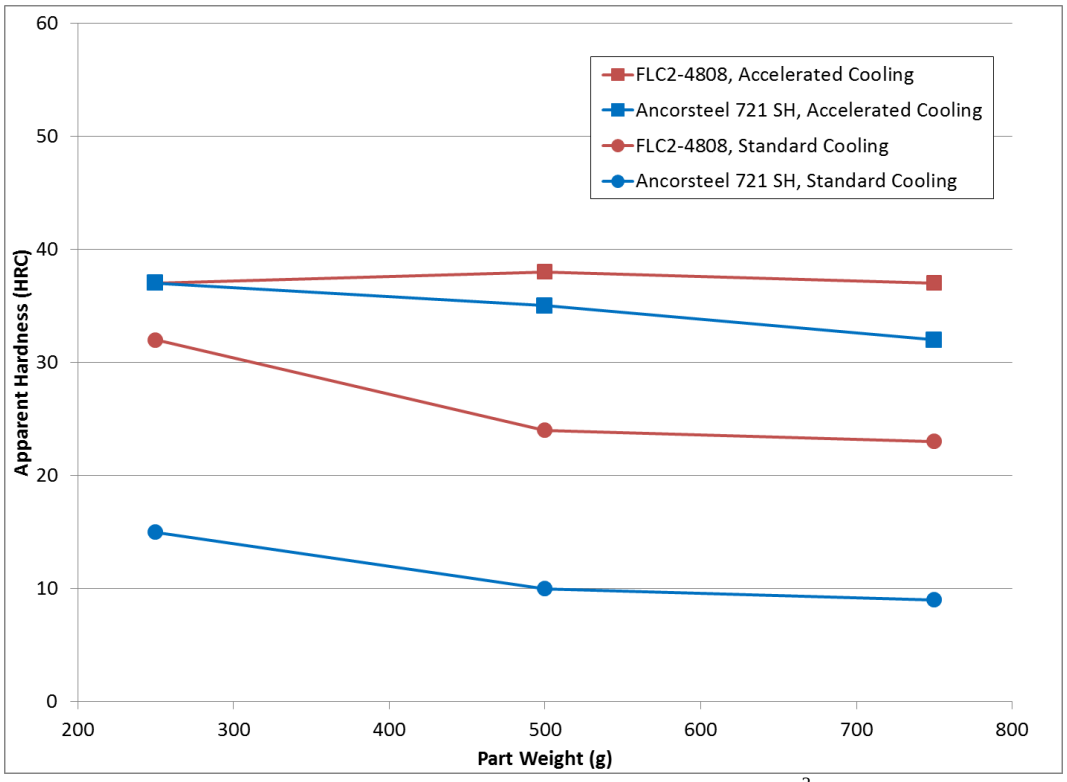

Figure 8: Apparent hardness of sprockets pressed to 7.0 g/cm^3 green density.

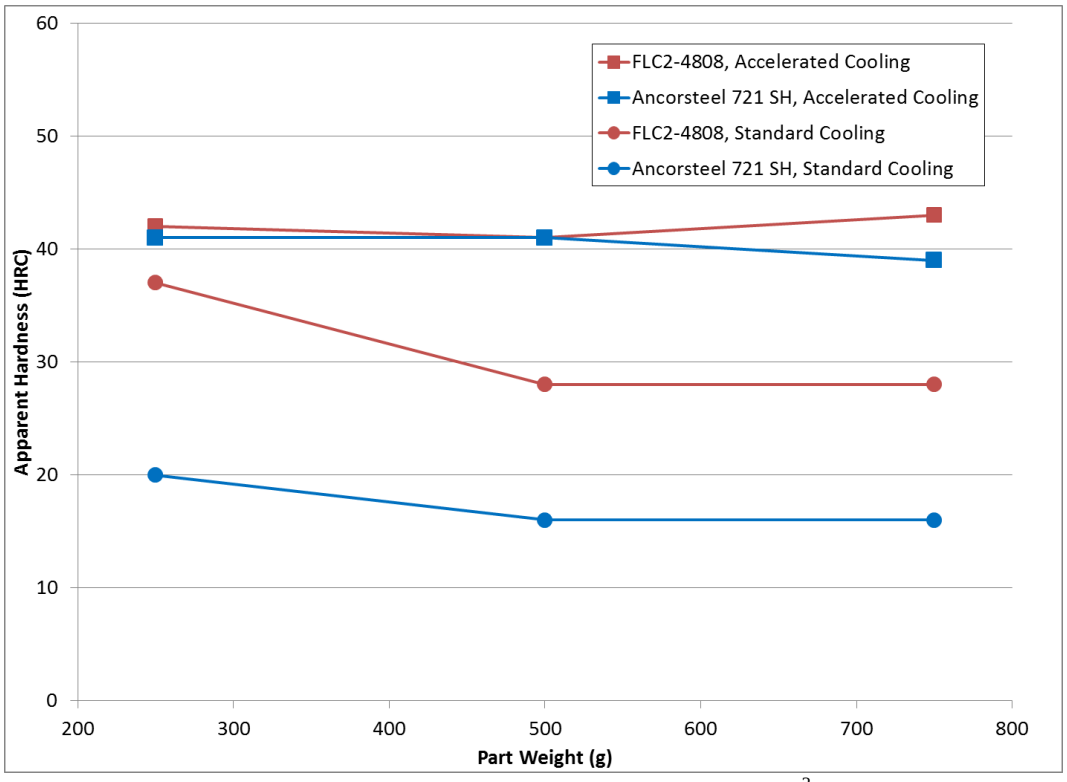

Figure 9: Apparent hardness of sprockets pressed to 7.2 g/cm^3 green density.

The etched microstructures of all the sprockets from this study can be seen in Figures 10 and 11. Figure 10 shows each of the sprockets in this study under standard cooling conditions. As indicated by the apparent hardness values in the previous figures, there is substantially more martensite in each of the sprockets made from FLC2-4808 using standard cooling. While there is a clear trend in both alloys of decreasing martensite content as sprocket weight increases, it is evident that even the largest sprocket made from FLC2-4808 has higher martensite content than the 250 g Ancorsteel 721 SH sprockets. The martensite percentage of each sample was also estimated via point count method and documented in Table 5. The FLC2-4808 was estimated to have a minimum of 40% martensite regardless of sample size at the standard cooling rate, while the Ancorsteel 721 SH had a maximum estimated martensite content of 28% in the smallest 250 g sprocket.

The sprockets in Figure 11 have microstructures that are far more homogeneous. These parts were all sintered using an accelerated cooling rate. All sprockets, regardless of alloy type or part size, were found to have over 90% martensite in the microstructure. Most of the sprockets show only small regions of bainite, with some larger bainitic islands appearing in the 750 g sprockets made from the Ancorsteel 721 SH base material.

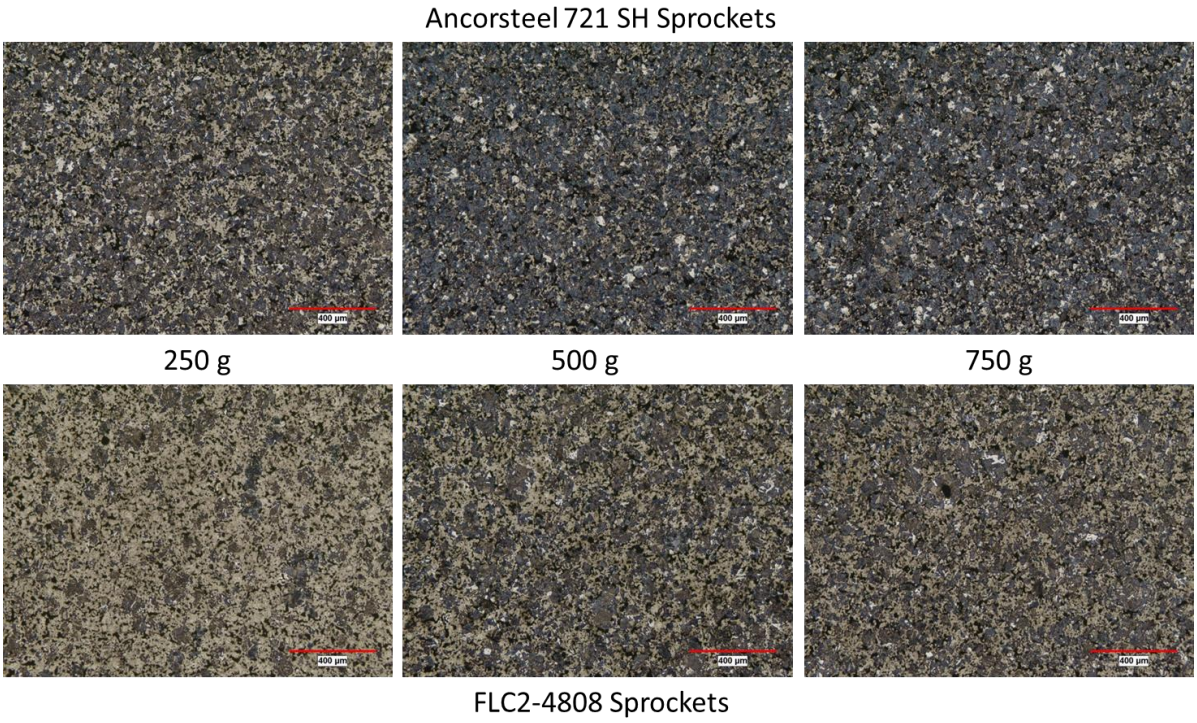

Figure 10: Etched core microstructures of Ancorsteel 721 SH and FLC2-4808 sprockets sintered with standard furnace cooling.

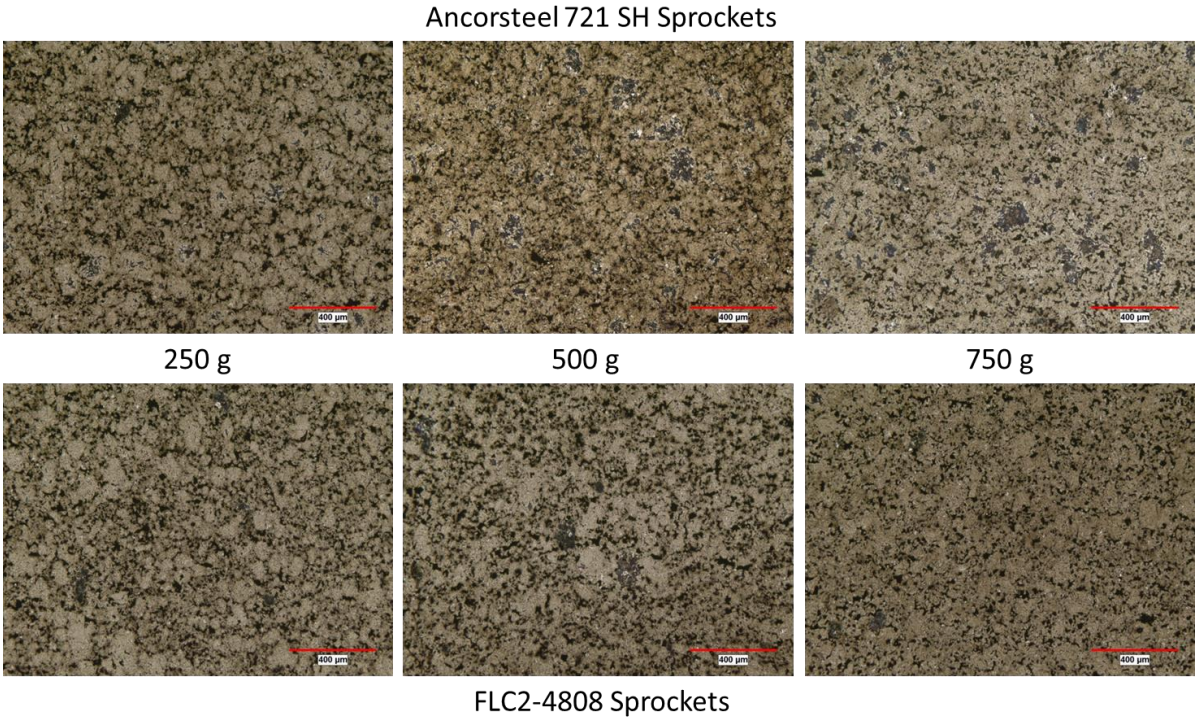

Figure 11: Etched core microstructures of Ancorsteel 721 SH and FLC2-4808 sprockets sintered with accelerated cooling.

Table 5: Estimated percent martensite in production trial sprockets compacted to 7.2 g/cm^3

Mix Designation	Part Weight (g)	Std. Cooling Martensite (%)	Acc. Cooling Martensite (%)
FLC2-4808	250	74	100
	500	42	98
	750	40	97
Ancorsteel 721 SH	250	28	98
	500	21	95
	750	15	92

To examine the relationship between apparent hardness measurement and etched microstructure, the estimated martensite percentage was plotted against the average apparent hardness for each set of sprockets at a 7.2 g/cm^3 density, regardless of all other variables. In Figure 12, it can be observed that the relationship between these two characteristics appears to be linear. This shows that apparent hardness can be achieved regardless of material, as long as the proper processing route is determined for a given part size and geometry.

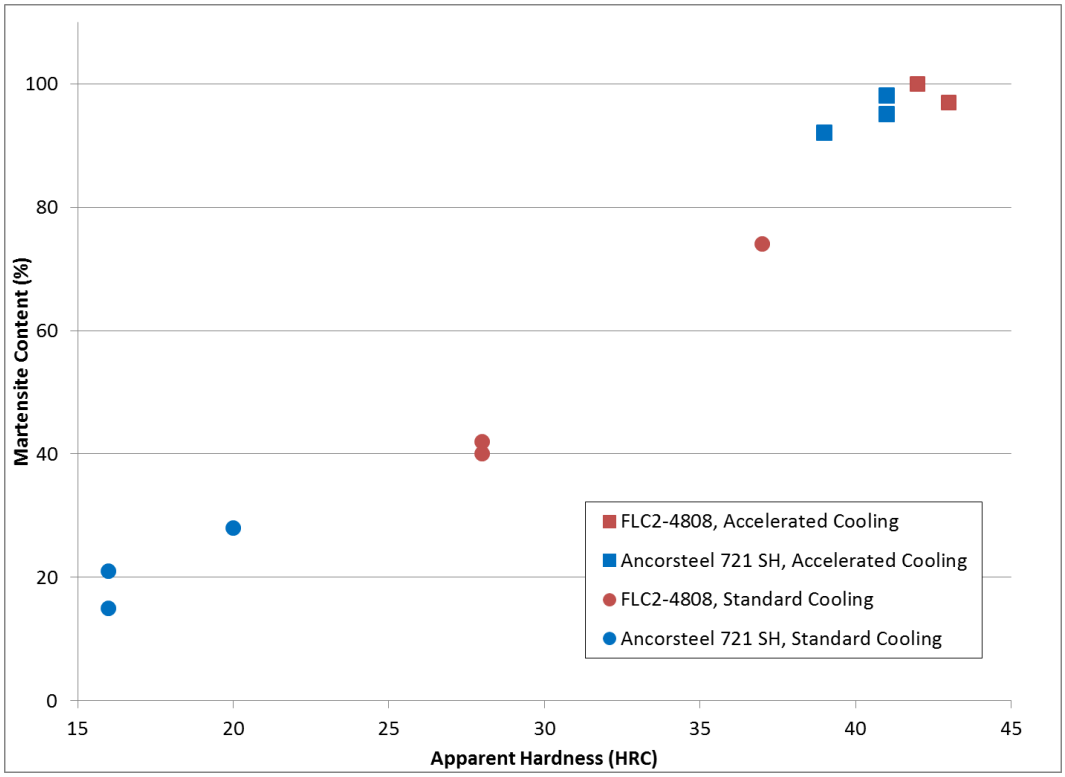

Figure 12: Relationship between martensite content and apparent hardness in 7.2 g/cm^3 density sprockets.

Conclusions

In summary, the material hardenability of FLC2-4808 and a leaner alloy was evaluated using laboratory samples and medium-sized sprockets under production conditions. The relationship between alloy content and cooling rate was examined in regards to resulting microstructure and corresponding apparent hardness. The following observations were made at the conclusion of this study:

- The combination of sinter-hardening alloys and high density processing allows for excellent mechanical strength and apparent hardness.
- FLC2-4808 is an extremely robust material, achieving high hardness and martensite content even at standard furnace cooling rates.
- Depending on alloy hardenability and cooling rate used, part size can have a substantial impact on the final properties and microstructure following sintering.
- Utilizing accelerated cooling allows for the potential to use leaner alloy selections to achieve comparable properties.
- The amount of martensite formed in the microstructure has a linear relationship to the apparent hardness of the final sintered component.

Acknowledgements

The authors wish to thank John Combs and Tihirah Harris for collecting the data, as well as Barry Diamond and Eric Alesczyk for contributing the photomicrographs presented within the manuscript.

References

1. M. Baran, A. Graham, A. Davala, R. Causton, and C. Schade, "A Superior Sinter-Hardenable Material", *Presented at PM^{2}TEC 1999, International Conference on Powder Metallurgy and Particulate Materials*, Vancouver, BC, Canada, June 20-24, 1999.
2. P. Sokolowski and B. Lindsley, "Influence of Chemical Composition and Austenitizing Temperature on Hardenability of PM Steels", *International Journal of Powder Metallurgy*, 2010, vol. 46, issue 1, pp. 43-54.
3. M. Marucci, G. Fillari, P. King, and K. Narasimhan, "A Review of Current Sinter-Hardening Technology", *Presented at PM2004 World Congress*, Vienna, Austria, August 25-28, 2004.
4. G. Fillari, R. Causton, and A. Lawley, "Effect of Cooling Rates During Sinter-Hardening", *Presented at PM^{2}TEC 2003, International Conference on Powder Metallurgy and Particulate Materials*, Las Vegas, Nevada, June 8-12, 2003.
5. D. Chasoglou, "High Performance PM Steels Through Sinter Hardening", *Presented at EURO PM 2017*, Milano, Italy, October 1-5, 2017.
6. S. Shah, G. Falleur, J. O'Brien, and F. Hanejko, "Cost-Effective, High Performance Lean Alloys", *Presented at PM2015 World Congress*, San Diego, California, May 17-20, 2015.
7. K. McQuaig and P. Sokolowski, "Hardenability Response of Lean Fe-Mo-Ni-C PM Alloys", *Presented at PM2012 International Conference on Powder Metallurgy and Particulate Materials*, Nashville, Tennessee, June 10-13, 2012.
8. F. Chagnon and Y. Trudel, "Optimizing Properties of PM Parts Through Selection of Proper Sinter Hardening Powder Grades", *Presented at PM^{2}TEC 2003, International Conference on Powder Metallurgy and Particulate Materials*, Las Vegas, Nevada, June 8-12, 2003.
9. F. Semel, "Cooling Rate Effects on the Metallurgical Response of a Recently Developed Sintering Hardening Grade", *Presented at PM^{2}TEC 2002, International Conference on Powder Metallurgy and Particulate Materials*, Orlando, Florida, June 16-21, 2002.
10. T. Haberberger, F. Hanejko, M. Marucci, P. King, "Properties and Applications of High Density Sinter-Hardening Materials", *Proceedings of the 2003 International Conference on Powder Metallurgy and Particulate Materials*, Las Vegas, Nevada, June 8-12, 2003.
11. M. Larsson and P. Knutsson, "Warm Die Compaction of High Density PM Components", *Presented at EURO PM 2017*, Milano, Italy, October 1-5, 2017.
12. F. Hanejko, "High Density via Single Pressing / Single Sintering", *Powder Metallurgy Technology*, 2010, vol. 28, no. 1, pp. 73-76.
13. Standard Test Methods for Metal Powders and Powder Metallurgy Products, published by MPIF, 2012.